UCLA

UCLA Previously Published Works

Title

INF2-Mediated Severing through Actin Filament Encirclement and Disruption

Permalink

https://escholarship.org/uc/item/0nh9200v

Journal

Current Biology, 24(2)

ISSN

0960-9822

Authors

Gurel, Pinar S

Ge, Peng

Grintsevich, Elena E

et al.

Publication Date

2014

DOI

10.1016/j.cub.2013.12.018

Peer reviewed

eScholarship.org Powered by the California Digital Library
University of California

Current Biology, Volume *24*

Supplemental Information

INF2-Mediated Severing through Actin Filament Encirclement and Disruption

Pinar S. Gurel, Peng Ge, Elena E. Grintsevich, Rui Shu, Laurent Blanchoin, Z. Hong Zhou, Emil Reisler, and Henry N. Higgs

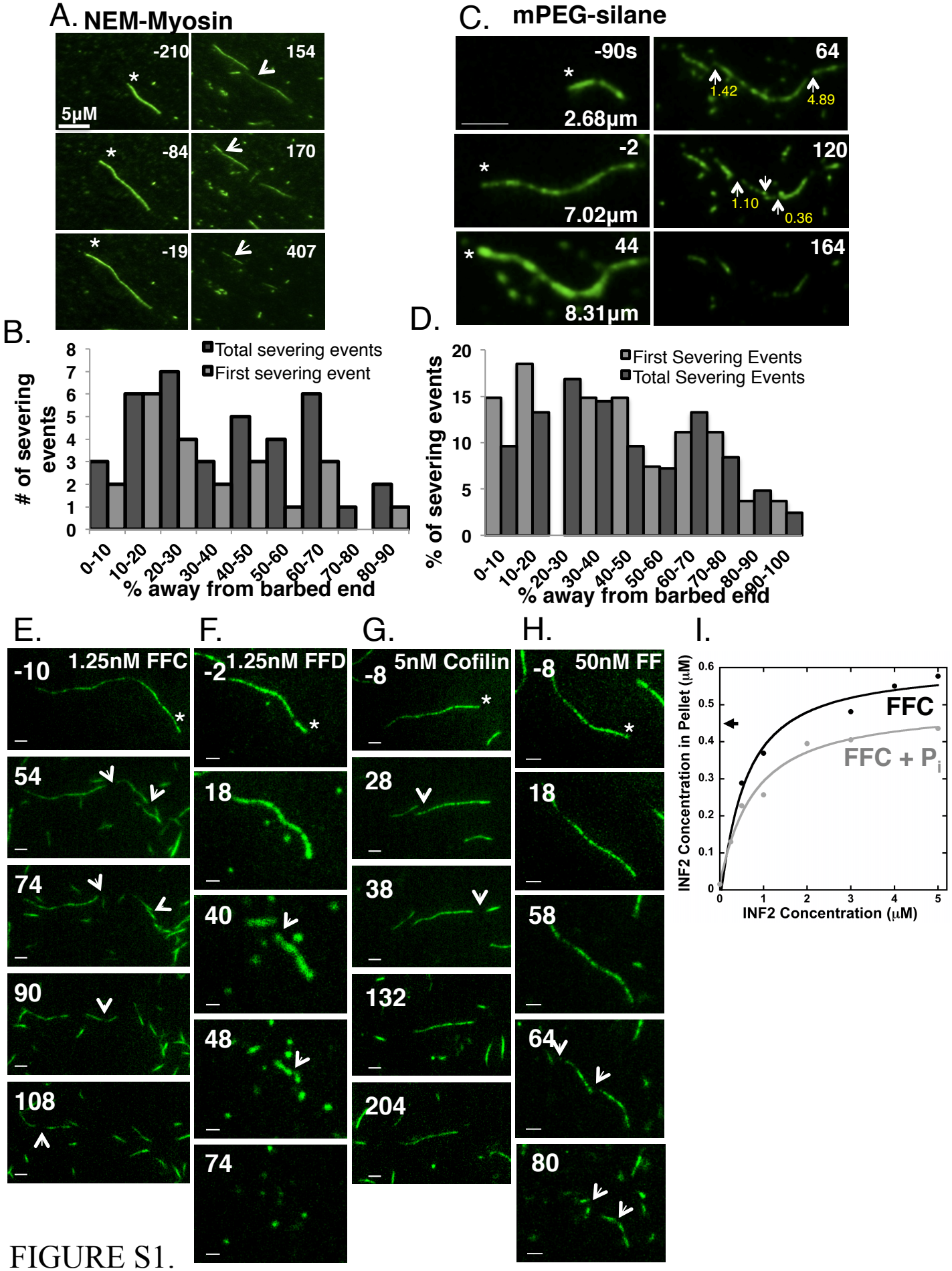
A. NEM-Myosin
-210
154
5μM
-84
170
-19
407
C. mPEG-silane
-90s
64
1.42
4.89
2.68μm
-2
120
7.02μm
1.10
0.36
44
164
8.31μm
B.
Total severing events
First severing event
# of severing events
% away from barbed end
D.
First Severing Events
Total Severing Events
% of severing events
% away from barbed end
E.
1.25nM FFC
F.
1.25nM FFD
G.
5nM Cofilin
H.
50nM FF
I.
FFC
FFC + Pi
INF2 Concentration in Pellet (μM)
INF2 Concentration (μM)

FIGURE S1.

Figure S1. INF2 severing and binding characteristics (related to Figure 1)

A. TIRF microscopy montage of INF2-FFC (10nM) with A488-labeled actin (20% A488-actin, starting 1 μM total actin) on NEM-myosin treated slides. Negative times represent filament elongating in absence of INF2, asterisk indicates barbed end, and arrows indicate severing events. . Actin monomers removed upon INF2 addition at time 0. Scale bar 5μm.

B. Histogram of severing event positions quantified from timecourses similar to A. Total of 22 filaments (59 severing events) were quantified with an average filament length of 15.6μm, range 9.9μm- 22.4μm at time = 0. Barbed end fragments were measured as a percentage of total filament length.

C. TIRF microscopy montage of INF2-FFC (10nM) severing actin (20% A488-actin, 1 μM starting actin concentration) on mPEG-silane treated slides. Negative times represent filament elongating in absence of INF2. Actin monomers removed upon INF2 addition at time 0. Asterisk indicates barbed end, arrows indicate severing events, severing position noted (μm from barbed end). Scale bar 2μm.

D. Histogram of severing event positions quantified from timecourses similar to C. Total of 17 filaments (84 severing events), were quantified with an average filament length of 7.6 μm, range 4.2μm- 14.8μm at time = 0. Barbed end fragments were measured as a percentage of total filament length.

E. TIRF microscopy montages of INF2-FFC (1.25nM) with A488-labeled actin (20% A488-actin, starting 1 μM total actin) on DDS/F127 treated slides. Representative examples from quantification of severing rate in figure 1G. Negative times represent filament elongating in absence of INF2, asterisk indicates barbed end, and arrows indicate severing events. Actin monomers were removed upon INF2 addition at time 0. Scale bar 2μm.

F. As in (A) but with INF2-FFD (1.25nM)

G. As in (A) but with cofilin (5nM)

H. As in (A) but with INF2-FF (50nM)

I. Cosedimentation assay using phalloidin-stabilized filaments (0.5 μM) incubated 5 min with indicated concentration of INF2-FFC in the absence or presence of 10mM phosphate. Arrow indicates concentration of actin in the pellet (0.45 μM).

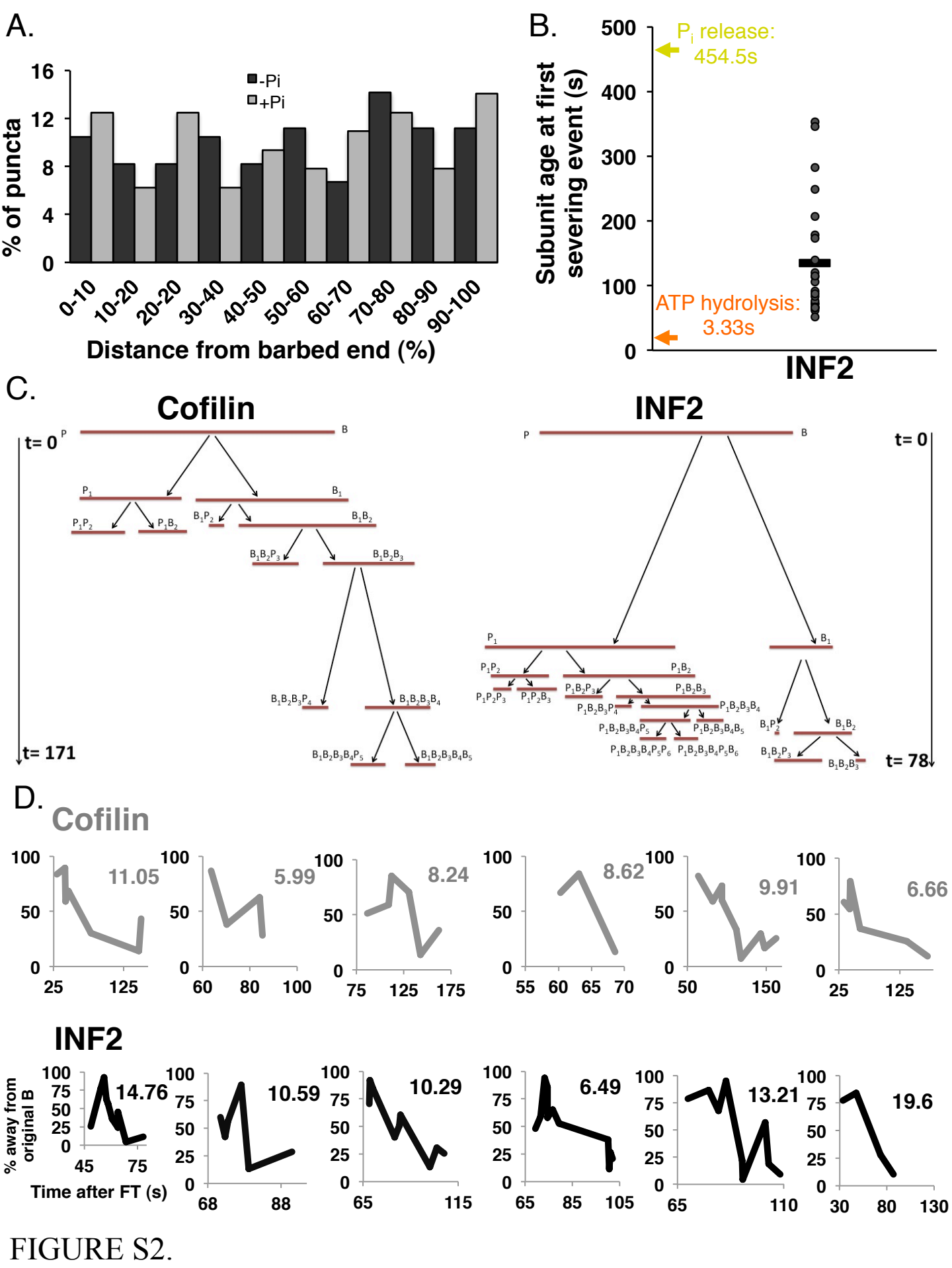
A.
% of puncta
16
12
8
4
0
-Pi
+Pi
0-10
10-20
20-20
30-40
40-50
50-60
60-70
70-80
80-90
90-100
Distance from barbed end (%)
B.
Subunit age at first severing event (s)
500
400
300
200
100
0
Pi release: 454.5s
ATP hydrolysis: 3.33s
INF2
C.
Cofilin
INF2
t= 0
t= 171
t= 78
D.
Cofilin
11.05
5.99
8.24
8.62
9.91
6.66
INF2
14.76
10.59
10.29
6.49
13.21
19.6
% away from original B
Time after FT (s)

FIGURE S2.

Figure S2. Quantification and omparison of INF2-FFC and cofilin-mediated severing (related to Figure 2)

A. Histogram of initial GFP-INF2-FFC puncta binding locations along filament +/- phosphate. n= 64 and 134 puncta (7 and 16 filaments) in the absence or presence of phosphate, respectively. Puncta were analyzed prior to severing and/or saturation, for 21.1-45.3s or 15.4-28.3s in the absence or presence of phosphate, respectively. Average filament length 12.6µm and 11.9µm (range 5.8-24.2µm and 6.3-19.6µm) in the absence and presence of phosphate respectively.
B. Quantification of subunit age at first severing event. Subunit ages were determined from filament elongation rate and location along filament where subunit was located at time of severing event (n=25 filaments). For comparison, subunits that should have undergone ATP hydrolysis and phosphate release are denoted in orange and yellow (respectively) . These values are based on expected rates from Blanchoin and Pollard 2002 Biochemistry, Carlier et al. 1998 FEBS letters.
C. Additional examples of tree maps diagraming severing events with time (sec) on the y-axis, from Figure 2E. t=0 denotes time of cofilin or INF2-FFC addition, B and P denote barbed and pointed ends respectively. Severed filament fragments are named based on severing history. 6.7 (cofilin) and 14.8 mm (INF2) filament represented, time and sizes drawn to scale.
D. Individual filaments monitored for severing position as a function of time after addition of INF2 or cofilin (six filaments for each). Y-axis values represent distance away from original filament barbed end, where total filament length = 100%. Starting filament lengths given in µm on each graph.

A.

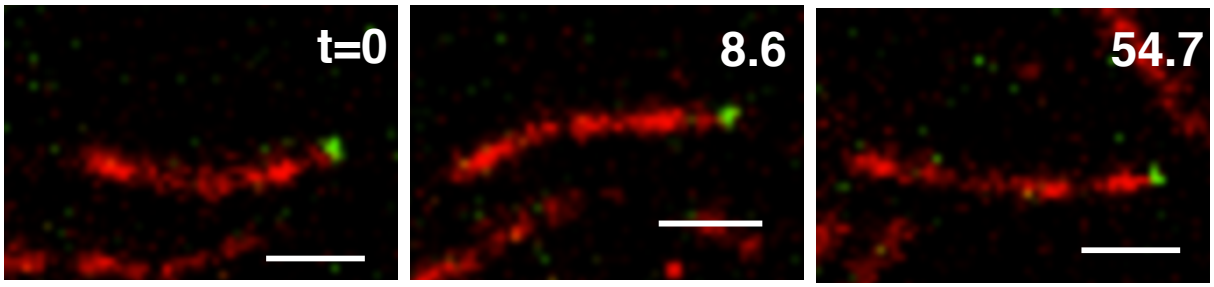
t=0
8.6
54.7

B.

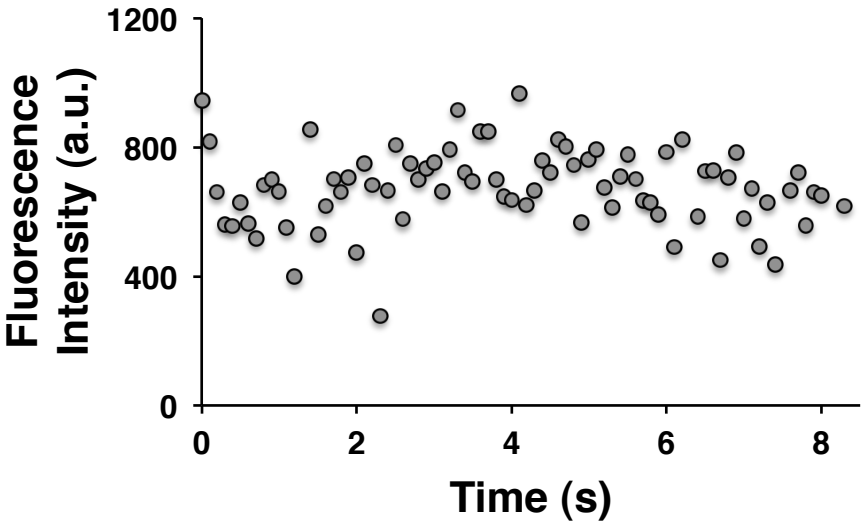
Fluorescence Intensity (a.u.)
1200
800
400
0
0
2
4
6
8
Time (s)

FIGURE S3.

Figure S3. INF2 processivity on filament barbed ends and calibration of single GFP fluorescence (related to Figure 3).

A. Two-color TIRF microscopy montage of actin monomers (1µM, 20% TAMRA) mixed with GFP-INF2-FFC (1nM) on DDS/F127-treated slides. INF2 is processively bound to elongating barbed end. Time is in sec. Scale bar 2µm.
B. Distribution of fluorescence intensity values for a SINGLE GFP-INF2 punctum at a filament barbed end quantified over time (83 frames, 8.3s, corresponding to filament in Figure 3C, right panel).

Table S1. INF2 binding affinities and stoichiometries from pelleting assays (related to Figure S1)

	K_d (μM)	Actin Binding Stoichiometry (INF2/Actin)
FFC	0.46	1.13
FFC + P_i	0.66	0.91
FF	2.8	0.8

Movie S1. GFP-INF2-FFC binding and severing actin filament. GFP-INF2 FFC (10nM) was added to TAMRA-actin filaments (1µM, 20% TAMRA initially) after allowing for polymerization for 7 minutes. GFP-INF2 puncta bind and then sever throughout filament. Movie corresponds to montage in Figure 1C and represents images taken 25s after GFP-INF2 FFC addition and actin monomer washout for a duration 54s. Dual-color simultaneous images were taken every 100ms and condensed to a 27s movie. Barbed end is on right, scale bar is 2µm.

Movie S2. GFP-INF2-FFC + 10mM phosphate binding actin filament. GFP-INF2 FFC (100nM) + 10mM P_i was added to TAMRA-actin filaments (1µM, 20% TAMRA initially) after allowing for polymerization for 7 minutes. GFP-INF2 puncta bind throughout the filament until saturation. Movie corresponds to montage in Figure 1D and represents images taken 10s after GFP-INF2 FFC + P_i addition and monomer washout for a duration of 35s. Dual-color simultaneous images were taken every 100ms and condensed to a 17s movie. Barbed end is on right, scale bar is 2µm.

Movie S3. A488-Cofilin binding and severing actin filament. A488-Cofilin (5nM) was added to TAMRA-actin filaments (1µM, 20% TAMRA initially) after allowing for polymerization for 7 minutes. A488-cofilin vectorially binds and severs aged filament regions. Movie corresponds to montage in Figure 1E and represents images taken for 40s immediately after A488-Cofilin addition and actin monomer washout. Dual-color simultaneous images were taken every 100ms and condensed to a 20s movie. Barbed end is on right, scale bar is 2µm.

Movie S4. A488-Cofilin + 10mM phosphate addition to actin. A488-Cofilin (100nM) + 10mM P_i was added to TAMRA-actin filaments (1µM, 20% TAMRA initially) after allowing for polymerization for 7 minutes. A488-cofilin binding to filaments in the presence of 10mM P_i is dramatically reduced. Movie corresponds to montage in Figure 1F and represents images taken for 57s immediately after A488-Cofilin + P_i addition and actin monomer washout. Dual-color simultaneous images were taken every 100ms and condensed to a 28s movie. Barbed end is on right, scale bar is 2µm.

Movie S5. Close-up of GFP-INF2-FFC puncta before and after a severing event- barbed end only. GFP-INF2 FFC (10nM) was added to TAMRA-actin filaments (1µM, 20% TAMRA initially) after allowing for polymerization for 7 minutes. A single GFP-INF2 punctum binds at a severing site, and then severs with punctum localization after severing event at newly formed barbed end only. Movie corresponds to montage in Figure 3C, right panel and represents images taken 25s after GFP-INF2 FFC addition for 14s immediately after GFP-INF2 FFC addition and actin monomer washout. Dual-color simultaneous images were taken every 100ms and condensed to a 9.8s movie. Barbed end is on right, scale bar is 2µm.

Movie S6. Close-up of GFP-INF2-FFC puncta before and after a severing event- barbed and pointed end. GFP-INF2 FFC (20nM) was added to TAMRA-actin filaments (1µM, 20% TAMRA initially) after allowing for polymerization for 7 minutes. A single GFP-INF2 punctum binds at severing site, and then severs with puncta localization after severing event at both newly formed barbed and pointed ends. Movie corresponds to montage in Figure 3C, left panel and represents images taken 24s after GFP-INF2 FFC addition and monomer washout for a duration of 8s. Dual-color simultaneous images were taken every 100ms and condensed to a 5.6s movie. Barbed end is on right, scale bar is 2µm.

Supplemental Experimental Procedures

DNA Constructs

Human INF2 ORF clone (CAAX variant, catalog number SC313010) was obtained from OriGene Technologies, Inc (Rockville, MD). INF2-FFC (amino acids 469-1249), INF2-FFD (amino acids 469-1015), and INF2-FF (469-941) were amplified using a GC-rich PCR system (Roche Applied Science) and subcloned into pGEX-KT vector [1] with a modified tobacco etch virus protease site for bacterial expression as a glutathione S-transferase fusion protein. GFP-fusions were made by cloning in PCR amplified INF2 into a pGEX-KT vector modified with eGFP. The GFP contained the A206K mutation, which reduces self-association dramatically [2].

Protein Preparation and Purification

All formin constructs were expressed in Rosetta2 E. coli (Stratagene Inc) as GST fusion proteins, following procedures used previously [3]. The constructs used were INF2-FFC (human CAAX variant, amino acids 469-1249), INF2-FF (human, 469-941), INF2-FFD (human, 469-1015), GFP-INF2-FFC, GFP-INF2-FF, FMNL3-FH2 (mouse), and mDia1-FH2 (mouse). Briefly, expression was induced in log phase cultures with 0.5 mM IPTG at 16˚C. After expression, extracts were passed over glutathione-Sepharose, cleaved with tobacco etch virus protease to elute the formin construct from GST, and further purified by ion exchange chromatography on SourceQ and/or gel filtration by Superdex200. All proteins were stored at -80°C in K50MEIDT. Rabbit skeletal muscle actin was purified from acetone powder [4] and labeled with pyrenyliodoacetamide [5], Alexa 488-succinimidyl ester (Invitrogen A20000) or TAMRA NHS ester (Invitrogen C1171) [6]. Both labeled and unlabeled actin were gel-filtered on

Supderdex200 and stored in G buffer at 4°C. Cofilin (budding yeast, D34C mutant) and Alexa488-labeled cofilin (maleimide link to cysteine 34) were expressed and purified as described previously [7].

Buffers

The following buffers were used frequently: G-buffer (2 mM Tris, pH 8, 0.5 mM DTT, 0.2 mM ATP, 0.1 mM $CaCl_2$, and 0.01% NaN_3), G-Mg buffer (same as G-buffer but with 0.1 mM $MgCl_2$ instead of $CaCl_2$), 10× K50MEI (500 mM KCl, 10 mM $MgCl_2$, 10 mM EGTA, and 100 mM imidazole, pH 7.0), 10× Na50MEI (same as 10× K50MEI but with 500 mM NaCl instead of KCl), and polymerization buffer (G-Mg buffer plus either 1× K50MEI or 1× Na50MEI and 0.5 mM thesit (the common name for the detergent nonaethylene glycol monododecyl ether (Sigma, P-9641), which was included to minimize protein adhesion to the tube/well). Polymerization buffer with 1× Na50MEI was used for pelleting assays because dodecyl sulfate precipitates as the potassium salt. Protein storage buffer (K50MEIDT) was composed of 1xK50MEI, 1mM DTT, 0.02% thesit. The TIRF buffer contained: 1xKMEI, 100mM DTT, 0.2mM ATP, 15mM Glucose, 0.5% Methyl Cellulose, 0.01mg/mL catalase (Sigma C3515), 0.05mg/mL glucose oxidase (Sigma G6125), 0.1% BSA). In cases of phosphate addition, 10 mM $NaPO_4$ pH 7.0 was added from a 500 mM stock.

TIRF Microscopy

Glass flow chambers were prepared from either VWR microcover glass (24x60mm No 1.5) and Gold Seal Rite-On micro slides (3x1 inch) or VWR microcover glasses (22x22mm and 18x18mm No 1.5) to hold 10μL volume. Three distinct methods for coverglass preparation were

used, described in turn below. Method 1: NEM-myosin. Flow chambers were formed then treated with 10nM N-ethylmaleimide treated rabbit skeletal muscle myosin (Cytoskeleton, Inc MY02) [8] for 1 minute. Chambers were then washed with high salt, BSA containing buffer (1% BSA, 50mM Tris, pH7.5, 600mM NaCl) to disassemble myosin aggregates, followed by low salt, BSA containing buffer (1% BSA, 50mM Tris, pH 7.5, 150mM NaCl) prior to use. Method 2: mPEG-Silane. Coverglasses were washed with acetone (30'), 96% ethanol (10'), RBS 35 detergent (Thermo 27952; 2 hours), and then water. Slides were dried with compressed airflow, incubated overnight with 5K mPEG-silane (Laysan Bio) at 1mg/mL in 96% ethanol, and then rinsed with 96% ethanol, followed by water. Chambers were washed with low salt, BSA containing buffer prior to use. Method 3: DDS/F127. Coverglasses were silanized using the procedure adapted from Gell et al. [9]. Briefly, coverglasses were washed in acetone (50'), ethanol (10'), water (1'), then incubated in Pirhana Solution (1:2 ratio of 30% H_2O_2 and H_2SO_4) for one hour. Glasses were then rinsed with water, 0.1M KOH, then water again and dried with inert gas before silanization. Glasses were silanized over night in a 0.0025% solution of dichlorodimethyl silane (Sigma 85126) in chloroform, then washed with methanol, dried with inert gas, and stored in clean sealed containers. For silanized cover glasses, chambers were incubated with 1% Pluronic F127 (Sigma P2443) in BRB80 buffer (80mM PIPES/KOH, pH 6.9, 1mM EGTA, 1mM $MgCl_2$) for 1 minute, then equilibrated in TIRF buffer.

For severing assays, 2μM actin (20% A488-labeled) in G-buffer was mixed with 2xTIRF buffer, flowed into the flow chamber, and polymerized for 7 minutes with monitoring on a Nikon Eclipse TE-2000 microscope with Nikon D-eclipse C1 488nm laser. At 7 min, 10μL formin or cofilin diluted in 1xTIRF buffer was flowed into the chamber, simultaneously washing out the

remaining actin monomers. Images were acquired every 2s with TIRF objective (60x 1.49 N.A.) and a Roper Cool-Snap camera.

Two-color Simultaneous TIRF Microscopy

For nucleation assays, unlabeled actin monomers were mixed with 20% TAMRA-labeled actin monomers in G-buffer, then diluted with 2xTIRF buffer without or with GFP-INF2 construct and flowed into the flow chamber. The filaments were visualized as quickly as possible (45-85s) on a Nikon Eclipse Ti-E inverted microscope with perfect focus and 488nm and 561nm laser. For severing assays, 2μM actin (20% TAMRA-labeled) in G-buffer was mixed with 2xTIRF buffer, flowed into the flow chamber, and polymerized for 7 minutes with monitoring. At 7 min, 10μL GFP-formin or A488-cofilin diluted in 1xTIRF buffer was flowed into the chamber, simultaneously washing out the remaining actin monomers. Simultaneous two-color images were acquired every 100ms with TIRF objective (60x 1.49 N.A.) and two iXON Ultra 897 cameras.

Image Analysis and Quantification of GFP-INF2 molecules per punctum

Images were processed and analyzed using Nikon NIS-Elements Software. For the determination of number of INF2 molecules per GFP punctum, single filament image sequences were background subtracted individually due to the variation in fluorescence intensity values throughout the field of view. Fluorescence intensity measurements were taken over 5-10 frames within 1-2 minutes of image sequence per diffraction-limited GFP punctum. Fluorescence intensity values were normalized to punctum area and averaged. Number of GFP-INF2

moleucles per punctum was determined by calibrating punctum fluorescence intensity values at the barbed end to represent 2 GFP-INF2 molecules (1 dimer).

Co-sedimentation Assays

Actin (4μM) was polymerized for 1h at 23°C in polymerization buffer (G-Mg buffer plus 1xNaMEI), followed by addition of 2.5x molar excess phalloidin. This actin stock was diluted to desired concentration in polymerization buffer in the absence or presence of formin, in polycarbonate 7x20mm centrifuge tubes (Beckman 343775) to a final volume of 200μL. Filaments were pipetted using cut pipetteman tips to minimize shearing. After 5 min at 23°C, samples were centrifuged at 80,000 rpm for 20 minutes at 4°C in a TLA-100.1 rotor (Beckman). 100μL of supernatant was removed and mixed with SDS-PAGE sample buffer. Pellets were washed briefly with 200μL 1xNaMEI, and then resuspended in 125μL SDS-PAGE sample buffer. Pellets were analyzed by Coomassie-stained SDS-PAGE and ImageJ software.

Negative Staining Electron Microscopy

To make negatively stained grids, actin (bare or INF2-FFC-decorated) samples are applied to EM grids with continuous carbon in 2.5 μL aliquots. In each grid, the applied sample is allowed to absorb to the grid for one minute, then blotted with a filter paper and stained by 6 μL 2.5% uranyl acetate solution for two minutes. Prepared grids are imaged in an FEI Tecnai F20 microscope operated at 200keV acceleration. Images are taken with a Tietz F415 CCD camera (TVIPS) at 50,000 nominal magnification, giving a calibrated pixel size of 2.216 Å. Filaments from the CCD frames are manually selected with EMAN [10] *helixboxer* module. Helical 3D

reconstructions are conducted with IHRSR [11] with EMAN as the reconstruction engine. Figures are prepared with UCSF Chimera [12].

Supplemental References

1. Hakes, D.J., and Dixon, J.E. (1992). New vectors for high level expression of recombinant proteins in bacteria. Anal Biochem *202*, 293-298.
2. Zacharias, D.A., Violin, J.D., Newton, A.C., and Tsien, R.Y. (2002). Partitioning of lipid-modified monomeric GFPs into membrane microdomains of live cells. Science *296*, 913-916.
3. Chhabra, E.S., and Higgs, H.N. (2006). INF2 Is a WASP homology 2 motif-containing formin that severs actin filaments and accelerates both polymerization and depolymerization. J Biol Chem *281*, 26754-26767.
4. Spudich, J.A., and Watt, S. (1971). The regulation of rabbit skeletal muscle contraction. I. Biochemical studies of the interaction of the tropomyosin-troponin complex with actin and the proteolytic fragments of myosin. J Biol Chem *246*, 4866-4871.
5. Cooper, J.A., Walker, S.B., and Pollard, T.D. (1983). Pyrene actin: documentation of the validity of a sensitive assay for actin polymerization. J Muscle Res Cell Motil *4*, 253-262.
6. Isambert, H., Venier, P., Maggs, A.C., Fattoum, A., Kassab, R., Pantaloni, D., and Carlier, M.F. (1995). Flexibility of actin filaments derived from thermal fluctuations. Effect of bound nucleotide, phalloidin, and muscle regulatory proteins. J Biol Chem *270*, 11437-11444.
7. Suarez, C., Roland, J., Boujemaa-Paterski, R., Kang, H., McCullough, B.R., Reymann, A.C., Guerin, C., Martiel, J.L., De la Cruz, E.M., and Blanchoin, L. (2011). Cofilin tunes the nucleotide state of actin filaments and severs at bare and decorated segment boundaries. Curr Biol *21*, 862-868.
8. Kovar, D.R., and Pollard, T.D. (2004). Insertional assembly of actin filament barbed ends in association with formins produces piconewton forces. P Natl Acad Sci USA *101*, 14725-14730.
9. Gell, C., Bormuth, V., Brouhard, G.J., Cohen, D.N., Diez, S., Friel, C.T., Helenius, J., Nitzsche, B., Petzold, H., Ribbe, J., et al. (2010). Microtubule dynamics reconstituted in vitro and imaged by single-molecule fluorescence microscopy. Methods Cell Biol *95*, 221-245.
10. Ludtke, S.J., Baldwin, P.R., and Chiu, W. (1999). EMAN: semiautomated software for high-resolution single-particle reconstructions. J Struct Biol *128*, 82-97.
11. Egelman, E.H. (2007). The iterative helical real space reconstruction method: surmounting the problems posed by real polymers. J Struct Biol *157*, 83-94.
12. Pettersen, E.F., Goddard, T.D., Huang, C.C., Couch, G.S., Greenblatt, D.M., Meng, E.C., and Ferrin, T.E. (2004). UCSF Chimera--a visualization system for exploratory research and analysis. J Comput Chem *25*, 1605-1612.